論文 / 著書情報
Article / Book Information

Title	TiO2 Composites for Efficient Poly(3-thiophene acetic acid) Sensitized Solar Cells
Authors	Younkyung Cho, Hyunho Kim, Minhak Oh, Myoung Soo Lah, Yutaka Majima, Kee-Sun Sohn, Myoungho Pyo
Citation	Journal of The Electrochemical Society, Vol. 158, No. , pp. B106-B111
発行日 / Pub. date	2010,
DOI	http://dx.doi.org/10.1149/1.3519305
権利情報 / Copyright	(c) The Electrochemical Society, Inc. 2010. All rights reserved. Except as provided under U.S. copyright law, this work may not be reproduced, resold, distributed, or modified without the express permission of The Electrochemical Society (ECS). The archival version of this work was published in Journal of The Electrochemical Society, Vol. 158, No. , pp. B106-B111

Journal of The Electrochemical Society, **158** (2) B106-B111 (2011)
0013-4651/2010/158(2)/B106/6/$28.00 © The Electrochemical Society

TiO_2 Composites for Efficient Poly(3-thiophene acetic acid) Sensitized Solar Cells

Younkyung Cho,[a,*] Hyunho Kim,[a] Minhak Oh,[b] Myoung Soo Lah,[b] Yutaka Majima,[a,c] Kee-Sun Sohn,[a] and Myoungho Pyo[a,z]

[a]*Department of Printed Electronics Engineering, Sunchon National University, Chonnam 540-742, Republic of Korea*
[b]*Interdisciplinary School of Green Energy, Ulsan National Institute of Science and Technology, Ulsan 689-798, Republic of Korea*
[c]*Materials and Structures Laboratory, Tokyo Institute of Technology, Yokohama 226-8503, Japan*

The effect of TiO_2 mesoporous structures sensitized with poly(3-thiophene acetic acid) (PTAA) on the photovoltaic performance was investigated. In contrast to conventional Ru-complex dye-sensitized solar cells (DSCs), the cell efficiency (η) of PTAA-sensitized solar cells exhibited strong dependence on the TiO_2 pore structures. Incorporation of up to 40 wt % large TiO_2 nanoparticles (L-TiO_2) into small TiO_2 nanoparticles (S-TiO_2) increased η, in spite of a reduction in dye loading due to a decrease in surface area. The highest η of $2.36 \pm 0.04\%$ was obtained for a TiO_2 film comprised of S-TiO_2 (60 wt %) and L-TiO_2 (40 wt %). Electrochemical impedance measurements suggested that the 25% increase in η for the DSC comprised of 40 wt % L-TiO_2 resulted not from rapid diffusion of the redox electrolyte through the larger pores, but instead was due to the higher electron density in the conduction band of TiO_2. It was inferred, therefore, that the highest η obtained for the DSC comprised of 40 wt % L-TiO_2 was due to the high degree of anchoring of COOH groups. This inference was further confirmed by obtaining an η of $2.92 \pm 0.06\%$, the highest η ever reported for a polymer-dye based DSC, using a low-molecular weight PTAA sensitizer.
 [DOI: 10.1149/1.3519305]

Manuscript submitted July 23, 2010; revised manuscript received November 1, 2010. Published December 2, 2010.

Since Grätzel and co-workers first reported a TiO_2 nanostructured photovoltaic device with an η of 7.1–7.9% under simulated solar light in 1991,[1] dye-sensitized solar cells (DSCs) have been extensively studied by numerous researchers to develop cost-effective photoelectrochemical devices as alternatives to Si-based solar cells.[2-4] As a result of continuous research activities during the past 20 years, DSCs with an η of approximately 11% have been achieved, which is comparable to the cell efficiency of amorphous Si-based solar cells.[5] In addition to their performance, another advantage of DSCs is that they are an optimal substitute for so-called building-integrated photovoltaic materials due to their colorful appearance and excellent transparency. However, the costs associated with large-scale production are prohibitive, requiring the replacement of expensive transition metal complex-based dyes with entirely organic materials.

In this respect, organic dyes have been the focus of an intensive investigation.[6-9] In addition to their cost-effectiveness, the absorption coefficient of organic dyes is 1 order of magnitude greater than that of conventional Ru-complex dyes. Indoline- and coumarin-based dyes are just two examples of organic dyes[7,8] with cell performance comparable to that of Ru-complex dyes.[9] Conjugated polymers with high absorption coefficients and tunable band levels ranging from visible to near-infrared absorption have also been examined as sensitizers in DSCs. A high density of anchoring groups of a polymer chain, which can offer better thermal stability than small-molecule sensitizers, may be another advantage of polymer dyes. Various polymers such as polyfluorene[10] and poly(arylene ethynylene)[11] have been used as DSC sensitizers. Among these conjugated polymers, thiophene-based polymers are the most widely studied.[12-14] In 2003, Yanagida et al. reported the highest efficiency of 2.4% with poly (3-thiophene acetic acid) (PTAA).[12,13] Since then, no work exceeded this value and typical η of polymer-dye-based DSCs was limited to 1.5% in most cases, requiring significant improvement of the cell performance in polymer-based DSCs.

In this paper, we describe the effects of TiO_2 particle size on PTAA-DSCs. We show that the η of a PTAA-DSC can be drastically increased by incorporating large TiO_2 nanoparticles (L-TiO_2) (140 nm) into conventional films comprised of small TiO_2 nanoparticles (S-TiO_2) (25 nm). To the best of our knowledge, this is the first report on the particle size dependence of polymer-based DSCs, although numerous studies on controlling the porosity of TiO_2 films have been reported.[15,16] In the present study, we also report that the η of a PTAA-DSC can be further increased to 2.9% by using low-molecular weight PTAA due to increased charge injection to TiO_2. This is the highest η reported for a polymer-dye-based DSC.

Experimental

PTAA was synthesized as reported previously.[17] Briefly, 3-thiopheneacetic acid (TAA, from Aldrich, USA) was converted into an ethyl ester form (TAEt) by refluxing an ethanol solution (10 mL) of TAA (2 g) and a few drops of concentrated H_2SO_4. After 24 h, the solvent was removed by evaporation. Precipitates were redissolved in methylether and impurities removed by H_2O extraction. TAEt was obtained as a brown liquid after methylether evaporation. For the polymerization of TAEt, 20 mL of a $CHCl_3$ solution of 0.5 M TAEt was added drop-wise to 30 mL $CHCl_3$ of 1.3 M $FeCl_3$ at 0°C. After 12 h, the polymer solution was poured into excess methanol and precipitates were washed with methanol. Finally, the TAEt polymer (0.8 g) was converted into PTAA by refluxing in a 2.0 M NaOH aqueous solution for 3 days. PTAA was obtained by slowly adding concentrated HCl to the soluble portion of the reaction mixture. The structure of PTAA was confirmed by ^{1}H NMR (DMSO-d_6, JEOL 400 M Hz); δ 7.2–7.3 ppm (m, 1 H), 12.5 ppm (s, 1 H), 3.5–3.9 ppm (m, 2 H). The weight average molecular weight (M_w) determined by gel permeation chromatography (PL-GPC110) was 18,000 g mol^{-1} (M_w/M_n = 1.8). Low-molecular weight PTAA was also synthesized by increasing the amount of $FeCl_3$ added during polymerization of TAEt (M_w = 4500 g mol^{-1}, M_w/M_n = 6.5).

TiO_2 pastes were prepared by dispersing TiO_2 nanopowders (1.0 g) in a poly(ethlene oxide) (PEO) solution (0.4 g PEO, 0.1 mL titanium tetraisopropoxide, 0.1 mL acetylacetone, 0.4 mL ethanol, 0.5 mL 1 M HNO_3, 2.1 mL H_2O) using a tip sonicator. The ratio of small-to-large TiO_2 nanoparticles, i.e., S-TiO_2 (P25, Degussa, Germany):L-TiO_2 (Sigma, USA), was varied as follows: 100:0, 80:20, 60:40, and 40:60. TiO_2 photoanodes were prepared on fluorine-doped tin oxide glass plates, which were O_3-cleaned and $TiCl_4$-treated, using a doctor blade technique. The TiO_2 film thickness was controlled by adjusting the adhesive tape thickness and the solid content of TiO_2 paste using ethanol. The coated electrodes

* Electrochemical Society Student Member.
z E-mail: mho@sunchon.ac.kr

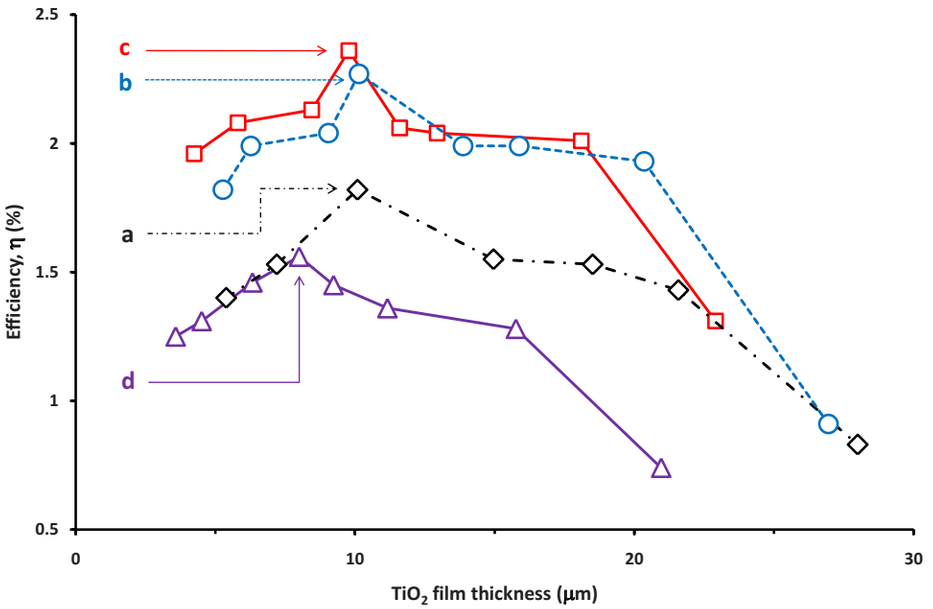

Figure 1. (Color online) Relationship between PTAA-DSC efficiency and TiO_2 film thickness. Photoanodes of DSC were made from different S-TiO_2:L-TiO_2 compositions of (a) 100:0, (b) 80:20, (c) 60:40, and (d) 40:60.

were sintered at 450°C for 30 min. The porous structure of the TiO_2 composites was examined by field-emission scanning electron microscope (FESEM) (S-4800 Hitachi, Japan). The thickness of the sintered films was measured using a surface profilometer (Nanoview 1000, Nano system). To quantify the surface area of the samples, N_2-sorption studies were performed on the samples using a BELSORP-max (BEL Japan, Inc.) by a standard volumetric technique at 77 K. The parts of the N_2-sorption isotherms in the P/P_0 range of 0.1–0.3 were fitted to the Brunauer-Emmett-Teller (BET) equation to determine the BET surface areas. All of the N_2-sorption isotherms were type II, but with small hysteresis at pressures close to the saturation point, which is typical for nonporous or macroporous material.

The adsorption of PTAA onto TiO_2 nanocrystalline electrodes was performed by immersing TiO_2 electrodes in dimethyl sulfoxide (DMSO) containing 10 mM PTAA at 20°C for 36 h. We found that adsorption times shorter than 36 h resulted in insufficient dye adsorption. After PTAA adsorption, the electrodes were repeatedly washed in flowing DMSO and ethanol to remove any loosely bound species on the surface of the electrode.

A sandwich cell was prepared using the dye adsorbed TiO_2 electrode and Pt counter electrode. A Surlyn film (SX 1170-60, Solaronix, Switzerland) with a hole of 0.20 cm^2 was affixed to a PTAA-adsorbed TiO_2 electrode with an active area of 0.196 cm^2 and was used as a spacer between the electrodes. The photoanode, together with the counter electrode, was heated at 125°C for 13 s to form a sealed cell. The iodine electrolyte was placed inside the cell utilizing capillary action through a predefined channel. A solar simulator (66984, Newport, USA), was focused to give 100 mW/cm^2, equivalent to 1 sun at AM 1.5. The short circuit photocurrent (J_{sc}) and the open circuit potential (V_{oc}) were measured using a potentiostat/galvanostat (Epsilon EC). Electrochemical impedance spectroscopy (EIS) measurements were carried out under the same experimental conditions by applying a 10 mV ac signal over the frequency range of 10^{-1}–10^5 Hz at V_{oc} using an impedance spectrometer (Parstat 2273). The incident photon-to-current efficiency (IPCE) was also compared in ac mode using an EQE-IPCE system (M-77890, Newport). The counter electrode was prepared by drop-coating a FTO glass plate with an ethanol solution of 5 mM H_2PtCl_6. The plates were air-dried for 5 min and then were heated at 400°C for 15 min. The iodide electrolyte used was comprised of 0.5 M tetrabutylammonium iodide, 0.05 M I_2, and 20 mM 1,2-dimethyl-3-propylimidazolium iodide in a mixed solvent of acetonitrile (60%) and ethylene carbonate (40%).

Results and Discussion

Figure 1 shows the relationships between η of PTAA-DSCs and the L-TiO_2 content and film thickness. The TiO_2 film thickness was controlled by use of adhesive tape and variation in the solid content of the paste as mentioned above. The photoanode with no L-TiO_2 resulted in the greatest η of 1.9% at a thickness of 10.5 μm (Fig. 1a). It is well-known that η increases with film thickness up to an optimal thickness and then decreases as film thickness continues to increase.[18] This behavior is also the case for polymer dye-sensitized solar cells. The maximal value of η reported in the present study was 1.9%, which is slightly lower than the reported value of 2.4%.[12,13] This difference in cell efficiency was likely due to the use of different electrolytes or to the M_w of PTAA. The incorporation of L-TiO_2 increased η substantially. Figures 1b and c show that η was enhanced by ca. 20% and 30% as a result of incorporation of 20 wt % and 40% L-TiO_2, respectively. Note that the film thickness with the highest η was ca. 10 μm as shown in Fig. 1a. A further increase of L-TiO_2 content, however, resulted in a significant reduction in cell performance with a maximal η of 1.6% at a thickness of 8.0 μm, as shown in Fig. 1d.

The photovoltaic properties of the PTAA-DSCs with the highest η for each composition are listed in Table I along with those of N3 dye-sensitized solar cells (N3-DSCs) for comparison. It is obvious that, unlike PTAA-DSC, the η of the N3-DSCs decreased as the L-TiO_2 content was increased. This result was expected since the incorporation of large-sized nanoparticles reduces the surface area for dye adsorption (see below). The increase in the cell performance of the PTAA-DSCs with up to 40 wt % L-TiO_2 is rather interesting.

When compared with the N3-DSCs, the lower V_{oc} of the PTAA-DSCs seems to be related to the shift of the conduction band of TiO_2 due to the protonation of TiO_2 surface.[19] This phenomenon was more prominent in polymer-DSCs since a substantial fraction of the polymer chain remained unanchored to the TiO_2 surface.[20] It should be mentioned that the addition of tetrabutyl pyridine (TBP) to increase V_{oc}[21] resulted in an η = 0.88% mainly due to J_{sc} reduction. This result suggests the presence of unanchored PTAA segments since deprotonation of the acidic moieties of PTAA upon addition of

Table I. Photovoltaic performances of PTAA-DSCs exhibiting the highest η for each TiO_2 composition and of N3-DSCs under the same conditions.

	PTAA[a]				N3[b]			
S-TiO_2:L-TiO_2	V_{oc} (V)	J_{sc} (mA cm^{-2})	FF[c] (%)	η (%)	V_{oc} (V)	J_{sc} (mA cm^{-2})	FF (%)	η (%)
100:0	0.50 ± 0.02	6.5 ± 0.2	64 ± 1	1.9 ± 0.1	0.76 ± 0.02	19.2 ± 0.1	69 ± 0	10.1 ± 0.2
80:20	0.51 ± 0.00	7.2 ± 0.5	62 ± 3	2.3 ± 0.1	0.76 ± 0.01	19.5 ± 0.3	67 ± 0	10.0 ± 0.2
60:40	0.52 ± 0.01	7.4 ± 0.3	62 ± 3	2.4 ± 0.0	0.79 ± 0.01	16.5 ± 0.0	68 ± 0	8.9 ± 0.1
40:60	0.50 ± 0.00	5.4 ± 0.1	59 ± 0	1.6 ± 0.0	0.77 ± 0.02	17.2 ± 0.0	65 ± 2	9.0 ± 0.1

[a] Three samples for each composition were tested.
[b] TiO_2 photoanodes showing the highest efficiency for PTAA-DSC were immersed in ethanol of 0.3 mM N3 for 18 h and 2 cells for each composition were tested.
[c] Fill factor.

basic TBP changes the chain conformation by disrupting conjugation.[22] In general, the η of the PTAA-DSCs were significantly less than the η of N3-DSCs, resulting from a reduction in J_{sc}. The variation of the η of the PTAA-DSCs with both L-TiO_2 content and film thickness was also closely related to the change in J_{sc}.

Because the increase in the η of PTAA-DSC with incorporation of L-TiO_2 might be due to enlarged pores, leading to faster diffusion of I_3^-, we first investigated the difference in pore size of the photoanodes using FESEM. Figure 2 shows the surface morphology of TiO_2 films comprised of S-TiO_2 and L-TiO_2 mixtures with weight ratios of (a) 100:0, (b) 80:20, (c) 60:40, and (d) 40:60. The TiO_2 nanoparticles were well distributed and pore size increased as the L-TiO_2 content increased. It should be mentioned, however, that the dependence of η on L-TiO_2 content was not due to the pore size effect (see below).

To compare the amount of PTAA dye adsorbed on TiO_2 of various compositions, thermogravimetric analysis was performed under air. Figure 3 (left) clearly indicates that the amount of PTAA adsorbed decreased as the L-TiO_2 content was increased. Based on the weight loss between 300 and 450°C and the PTAA ashes remaining at 650°C, the number of moles of PTAA-repeating units adsorbed on 1 g of TiO_2 was calculated. Table II shows that the amount adsorbed on 1 g of TiO_2 gradually decreased from 1.05 mmole to 0.662 mmole as the L-TiO_2 content was increased (3rd column). Because the total weight of TiO_2 adsorbed for a single cell also decreased, as shown in the 4th column of Table II, the total PTAA adsorbed for a single cell decreased more rapidly with the increase in L-TiO_2 content, as shown in the 5th column of Table II. The total amount (weight) of TiO_2 deposited per a single photoanode was averaged for 42 single cells since the weight difference of a single photoanode before and after TiO_2 coating was too small to directly measure. BET measurements (Table II, 6th column) suggest that the surface area available for PTAA adsorption was reduced, with increasing L-TiO_2 content. Since the reduction of the surface area available for PTAA adsorption with the incorporation of L-TiO_2 is more conspicuous than that for the total PTAA adsorbed in a single cell, PTAA adsorbed per unit surface area became greater (Table II, 7th column). Note that the amount of PTAA per unit surface area is ca. 2 orders of magnitude smaller than 10^{-3} mol m^{-2} of N3 dye adsorbed on TiO_2.[23]

It is interesting that, in spite of the decrease of the total PTAA adsorbed, the power conversion efficiency was enhanced by incorporation of L-TiO_2 into PTAA-DSCs containing up to 40 wt % L-TiO_2. This result implies that the incorporation of PTAA into TiO_2 nanostructures does not necessarily result in the involvement

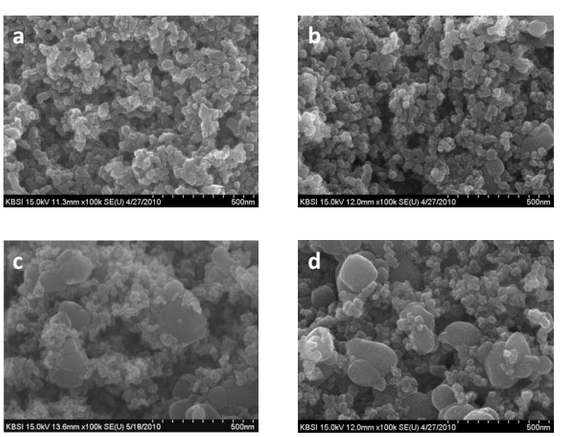

Figure 2. FESEM images of TiO_2 films comprised of S-TiO_2 and L-TiO_2 with ratios of (a) 100:0, (b) 80:20, (c) 60:40, and (d) 40:60.

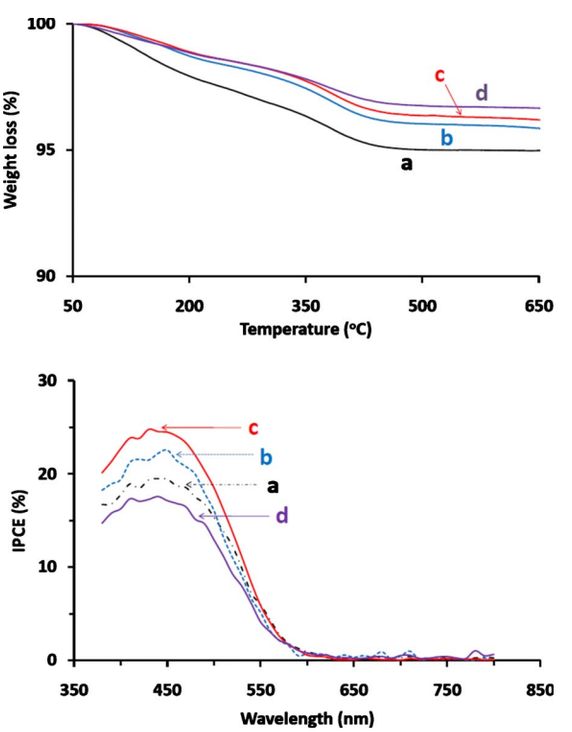

Figure 3. (Color online) (left) Thermogravimetric analysis of PTAA-adsorbed TiO_2 in air at 10°C min^{-1}. (right) IPCE of PTAA-DSCs fabricated from photoanodes comprised of S-TiO_2 and L-TiO_2. The S-TiO_2 to L-TiO_2 were (a) 100:0, (b) 80:20, (c) 60:40, and (d) 40:60.

Table II. Characteristics of photoanodes exhibiting the highest η for each composition.

S-TiO_2:L-TiO_2	Thickness[a] (μm)	PTAA adsorbed on g TiO_2[b] (mole g^{-1})	TiO_2 used for photoanode (g)	Total PTAA adsorbed in a single cell (mole)	Specific surface area[c] (m^2 g^{-1})	PTAA adsorbed per unit surface (mole m^2)	Pore volume[d] (cm^3 g^{-1})
100:0	10.5	1.05×10^{-3}	0.300×10^{-3}	3.15×10^{-7}	131	0.802×10^{-5}	0.43
80:20	10.1	0.843×10^{-3}	0.276×10^{-3}	2.33×10^{-7}	52.7	1.59×10^{-5}	0.46
60:40	9.8	0.775×10^{-3}	0.240×10^{-3}	1.86×10^{-7}	47.9	1.62×10^{-5}	0.54
40:60	8.0	0.662×10^{-3}	0.190×10^{-3}	1.26×10^{-7}	31.9	2.08×10^{-5}	0.57

[a] Measured by profilometry.
[b] Obtained from thermogravimetric analysis.
[c] BET measurements for N_2 adsorption.
[d] Determined from volume and weight of TiO_2 films and density of anatase.

of entire segments of PTAA in the photon-to-electricity conversion process. The degree of anchoring seems to increase with L-TiO_2 with a concurrent increase in pore volume (Table II, last column). Increased pore volumes can provide the polymer chains more flexibility, leading to greater opportunities for anchoring during adsorption. However, the low total PTAA loading in the PTAA-DSC comprised of 60 wt % L-TiO_2 resulted in the lowest η.

IPCE spectra measured for the PTAA-DSCs with the best η at each composition are shown in Fig. 3 (right). As expected from cell performance, the IPCE measurements also indicated that the PTAA-DSC comprised of 40 wt % L-TiO_2 has the highest efficiency, while the lowest efficiency was observed for the PTAA-DSC with 60 wt % L-TiO_2. No distinct shift in the maximum conversion wavelength was observed.

An EIS investigation was carried out to evaluate both electron transport and I_3^- diffusion. Figure 4 illustrates impedance changes of the PTAA-DSCs with the best η at each composition with ac modulation (±10 mV, 10^{-1}–10^5 Hz) at V_{oc}. The semicircles in the high and low frequency region, which correspond to the impedances of the electron transfer at the Pt counter electrode and I_3^- diffusion, respectively, were similar.[24,25] The detectable differences that were evident in the middle frequency region are indicative of the different charge transfer kinetics at the TiO_2/PTAA/electrolyte interface. As an increase of the L-TiO_2 content, the radius of the semicircle in the middle frequency region becomes smaller up to 40 wt % L-TiO_2. The inset of Fig. 4, which depicts the EIS spectra of N3-DSC, reveals an opposite behavior that the radius gradually increases in the middle frequency region with an increase in the L-TiO_2 content. This result excludes the possibility that the variation of the η of PTAA-DSCs with L-TiO_2 content was due to different TiO_2 nanostructures, such as a different degree of necking between TiO_2 nanoparticles.

We analyzed the EIS spectra based on the transmission line model proposed by others.[26-29] The dashed lines in Fig. 4 represent the simulation curves. The charge transfer resistance (R_k) and the chemical capacitance (C_μ) obtained were listed in Table III. It is interesting that R_k is the smallest at the L-TiO_2 of 40 wt %, meaning that the recombination of electrons in conduction band to I_3^- is least hampered. This might attribute to the local I_3^- concentration. As mentioned above, efficient involvement of PTAA in the photon-current conversion process at the L-TiO_2 of 40 wt % can lead to high local $[I_3^-]$. The lowest R_k at the L-TiO_2 of 40 wt % is compensated by the highest C_μ resulting in the longest lifetime of electrons ($R_k \cdot C_\mu$) of 0.077 s. The change of total electron density in TiO_2 (n) also supports our inference, which is related to C_μ by

$$n = (C_\mu \cdot k_B \cdot T)/(q^2 \cdot A \cdot L)$$

where k_B, T, q, A, and L represent Boltzmann constant (1.381×10^{-23} J K^{-1}), absolute temperature (293 K), charge of an electron (1.6×10^{-19} C), the electrode area (0.196 cm^2), and the TiO_2 film thickness (cm), respectively.[26] The PTAA-DSC with 40 wt %

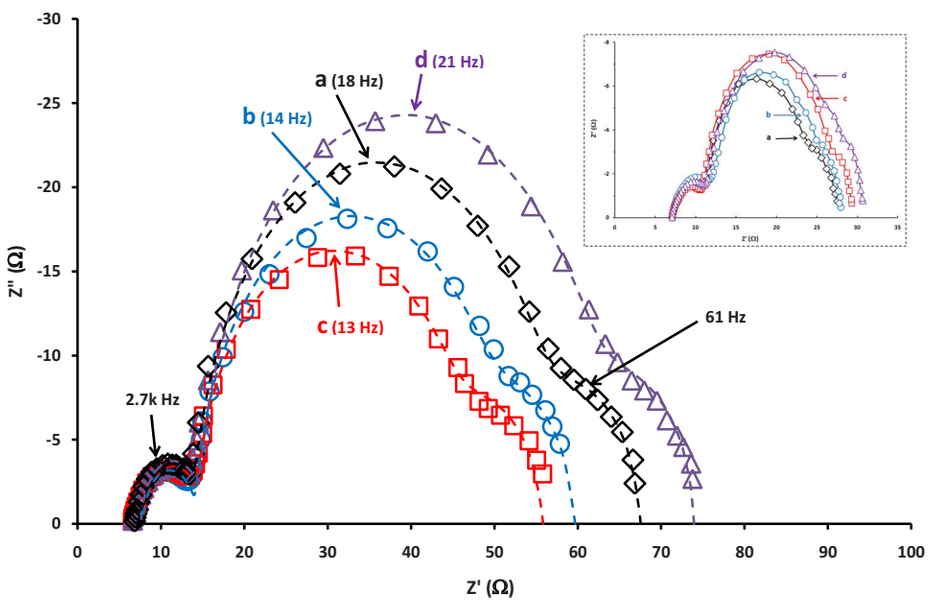

Figure 4. (Color online) EIS spectra of PTAA-DSCs under illumination. Photoanodes were comprised of S-TiO_2 and L-TiO_2 with ratios of (a) 100:0, (b) 80:20, (c) 60:40, and (d) 40:60. ac potential of ±10 mV at V_{oc} was applied in a frequency range of 10^{-1}–10^5 Hz. For comparison, EIS spectra of N3-DSC are shown in the inset.

Table III. Charge transfer parameters of PTAA-DSCs determined from EIS spectra.

S-TiO_2:L-TiO_2	Charge transfer resistance related to recombination, R_k (Ω)	Chemical capacitance, C_μ (mF)	Characteristic time constant (s)	Total electron density in TiO_2 (cm^{-3})	Diffusion coefficient of I_3^- ($cm^2\ s^{-1}$)
100:0	40.0	1.4	0.056	1.07×10^{18}	1.0×10^{-5}
80:20	33.5	2.1	0.071	1.68×10^{18}	1.1×10^{-5}
60:40	29.5	2.6	0.077	2.11×10^{18}	0.9×10^{-5}
40:60	45.5	1.0	0.048	1.06×10^{18}	1.2×10^{-5}

L-TiO_2 showed a total electron density that was twofold greater than that of the PTAA-DSC with no L-TiO_2, although the total dye loading was less than that of the other DSCs (except the PTAA-DSC comprised of 60 wt % L-TiO_2). This result clearly suggests that only some of the PTAA within the TiO_2 nanoporous structure is involved in the photoconversion process. However, a greater fraction of the PTAA can contribute to light harvesting as the L-TiO_2 content increases. This is because the large pore volumes induced by L-TiO_2 incorporation enhance more polymer chain flexibility, resulting in the increasing chance of covalent bonding of COOH moieties to TiO_2. The diffusion coefficients of I_3^- obtained from the curve fitting did not substantially vary with L-TiO_2 content, as expected from the EIS spectra.

In order to further rationalize this inference, we synthesized PTAA of a lower molecular weight PTAA for use in a preliminary examination. The cell performance of the DSC sensitized with the low-molecular weight PTAA was compared with that of its high-molecular weight counterpart. Figure 5 shows the current–voltage (J-V) curves of the PTAA-DSCs with the 40 wt % L-TiO_2 photoanode sensitized by PTAA of M_w of (a) 18,000 g mol^{-1} and (b) 4500 g mol^{-1}. Clearly, J_{sc} increased due to efficient charge injection, which resulted from greater anchoring of PTAA of the low-molecular weight PTAA. The absorption spectra of PTAA in DSC revealed slight peak broadening due to greater polydispersity ($M_w/M_n = 6.5$) of low-molecular weight PTAA, but the total absorptions were similar.

Conclusions

PTAA (M_w = 18,000 g mol^{-1}) was adsorbed onto TiO_2 photoanodes of various compositions. L-TiO_2 was incorporated into S-TiO_2 to be 0, 20, 40, and 60 wt %. Cell performance was enhanced by addition of L-TiO_2 up to 40 wt %. The cell efficiency (η) of 1.9% for the PTAA-DSC with a photoanode without L-TiO_2 was increased to 2.4% for the PTAA-DSC with a 40 wt % L-TiO_2 photoanode. However, when the L-TiO_2 content was 60 wt %, η decreased to 1.6%. EIS analysis revealed that the increase in η was not due to accelerated I_3^- diffusion through the large pores produced by L-TiO_2, but to enhanced anchoring of PTAA to TiO_2, though PTAA-dye loading was decreased by incorporation of L-TiO_2. This was further validated by investigating PTAA-DSC sensitized with low-molecular weight PTAA (M_w = 4500 g mol^{-1}). An η of 2.92 ± 0.06% was obtained using low-molecular weight PTAA which is the highest value ever reported for polymer-dye sensitized solar cells.

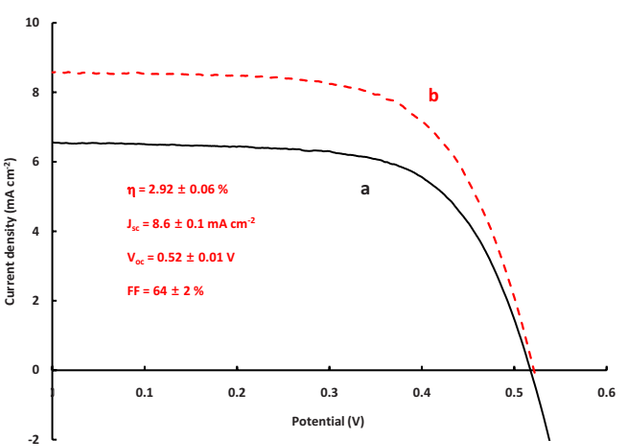

Figure 5. (Color online) J-V curves of PTAA-DSCs equipped with 40 wt % L-TiO_2 photoanodes sensitized by PTAA of M_w of (a) 18,000 and (b) 4500 g mol^{-1}.

Acknowledgments

This research was supported in part by the WCU (World Class University) program at Sunchon National University. This work was also supported in part by the project of Regional Innovation Center (RIC) at Sunchon National University and by the Ministry of Education, Science Technology (MEST) and Korea Institute for Advancement of Technology (KIAT) through the Human Resource Training Project for Regional Innovation.

Sunchon National University assisted in meeting the publication costs of this article.

References

1. B. O'Regan and M. Grätzel, *Nature (London)*, **353**, 737 (1991).
2. B. E. Hardin, E. T. Hoke, P. B. Armstrong, J.-H. Yum, P. Comte, T. Torres, J. M. J. Fréchet, M. K. Nazeeruddin, M. Grätzel, and M. D. McGehee, *Nat. Photonics*, **3**, 406 (2009).
3. P. Chen, J.-H. Yum, F. D. Angelis, E. Mosconi, S. Fantacci, S.-J. Moon, R. H. Baker, J. Ko, M. K. Nazeeruddin, and M. Grätzel, *Nano Lett.*, **9**, 2487 (2009).
4. C. Xu, P. H. Shin, L. Cao, J. Wu, and D. Gao, *Chem. Mater.*, **22**, 143 (2010).
5. M. Grätzel, *Nature (London)*, **414**, 338 (2001).
6. K. Hara, T. Sato, R. Katoh, A. Furube, T. Yoshihara, M. Murai, M. Kurashige, S. Ito, A. Shinpo, S. Suga, et al., *Adv. Funct. Mater.*, **15**, 246 (2005).
7. T. Horiuchi, H. Miura, K. Sumioka, and S. Uchida, *J. Am. Chem. Soc.*, **126**, 12218 (2004).
8. Z.-S. Wang, Y. Cui, Y. Dan-oh, C. Kasada, A. Shinpo, and K. Hara, *J. Phys. Chem. C*, **111**, 7224 (2007).
9. S. Ito, H. Miura, S. Uchida, M. Takada, K. Sumioka, P. Liska, P. Comte, P. Péchy, and M. Grätzel, *Chem. Commun. (Cambridge)*, **2008**, 5194.
10. X. Liu, R. Zhu, Y. Zhang, B. Liu, and S. Ramakrishna, *Chem. Commun. (Cambridge)*, **2008**, 3789.
11. H. Jiang, X. Zhao, A. H. Shelton, S. H. Lee, J. R. Reynolds, and K. S. Schanze, *ACS Appl. Mater. Interf.*, **1**, 381 (2009).
12. G. K. R. Senadeera, K. Nakamura, T. Kitamura, Y. Wada, and S. Yanagida, *Appl. Phys. Lett.*, **83**, 5470 (2003).
13. S. Yanagida, G. K. R. Senadeera, K. Nakamura, T. Kitamura, and Y. Wada, *J. Photochem. Photobiol., A*, **166**, 75 (2004).
14. J. K. Mwaura, X. Zhao, H. Jiang, K. S. Schanze, and J. R. Reynolds, *Chem. Mater.*, **18**, 6109 (2006).
15. H.-J. Koo, J. Park, B. Yoo, K. Yoo, K. Kim, and N. G. Park, *Inorg. Chim. Acta*, **361**, 677 (2008).
16. K.-M. Lee, V. Suryanarayanan, and K.-C. Ho, *J. Power Sources*, **188**, 635 (2009).
17. B. S. Kim, L. Chen, J. Gong, and Y. Osada, *Macromolecules*, **32**, 3964 (1999).
18. Z.-S. Wang, H. Kawauchi, T. Kashima, and H. Arakawa, *Coord. Chem. Rev.*, **248**, 1381 (2004).
19. M. K. Nazeeruddin, S. M. Zakeeruddin, R. Humphry-Baker, M. Jirousek, P. Liska, N. Vlachopoulos, V. Shklover, C.-H. Fischer, and M. Grätzel, *Inorg. Chem.*, **38**, 6298 (1999).
20. V. S. Saji, K. Zong, and M. Pyo, *J. Photochem. Photobiol., A*, **212**, 81 (2010).
21. M. K. Nazeeruddin, A. Kay, I. Rodicio, R. Humpbry-Baker, E. Miiller, P. Liska, N.

Vlachopoulos, and M. Grätzel, *J. Am. Chem. Soc.*, **115**, 6382 (1993).
22. T.-Q. Nguyen and B. J. Schwartz, *J. Chem. Phys.*, **116**, 8198 (2002).
23. J. A. Pollard, D. Zhang, J. A. Downing, F. J. Knorr, and J. L. McHale, *J. Phys. Chem. A*, **109**, 11443 (2005).
24. R. Kern, R. Sastrawan, J. Ferber, R. Stangl, and J. Luther, *Electrochim. Acta*, **47**, 4213 (2002).
25. M. Adachi, M. Sakamoto, J. Jiu, Y. Ogata, and S. Isoda, *J. Phys. Chem. B*, **110**, 13872 (2006).
26. F. Fabregat-Santiago, J. Bisquert, G. Garcia-Belmonte, G. Boschloo, and A. Hagfeldt, *Sol. Energy Mater. Sol. Cells*, **87**, 117 (2005).
27. A. Hagfeldt and L. Peter, in *Dye-Sensitized Solar Cells*, Chap. 10, K. Kalyanasundaram, Editor, EPFL Press, Switzerland (2010).
28. J. Bisquert and F. Fabregat-Santiago, in *Dye-Sensitized Solar Cells*, Chap. 12, K. Kalyanasundaram, Editor, EPFL Press, Switzerland (2010).
29. F. Fabregat-Santiago, H. Randriamahazaka, A. Zaban, J. Garcia-Cañadas, G. Garcia-Belmonte, and J. Bisquert, *Phys. Chem. Chem. Phys.*, **8**, 1827 (2006).